An experimental FTIR-ATR and computational study of H-bonding in ethanol/water mixtures

Constantinos D. Zeinalipour-Yazdi*[a,b], Eriketi Z. Loizidou[b]

[a] *School of Health, Sport and Bioscience, University of East London, Stratford Campus, Water Lane, London E15 4LZ, UK*

[b] *Department of Natural Sciences, Middlesex University, Hendon Campus, The Burroughs, London, NW4 4BT, UK*

*Correspondence to: c.zeinalipour-yazdi@uel.ac.uk

Abstract

Ethanol/water mixtures have served as a model to study the hydrophobic effect and the formation of clathrate and other cage like water formations around the hydrophobic end of ethanol. We have studied the evolution of FTIR-ATR spectra of ethanol/water mixtures as a function of the content of water in the mixture. The experimental spectra show redshift of primarily the H-O-H bending vibration, which is 18.9 cm^{-1} in total width. It also shows a blueshift of 9.0 cm^{-1} of the asymmetric stretching vibration of C-H groups of β-CH_3. These infrared spectral shifts are consistent with the formation of a cyclic H-bonded network between ethanol and H-bonded water molecules. This hypothesis has been supported by full optimizations of high-level B3LYP/aug-cc-pVQZ calculations in implicit and explicit water and ethanol solvents as well as MMFF94s simulations of ethanol in explicit water clusters with up to 30 water molecules.

Keywords: Hydrophobic effect, ethanol/water mixtures, H-bonded networks, Alcohol binary mixtures

1. Introduction

The study of the solvation of ethanol in water is of fundamental importance in many fields of science.[1-3] The formation of solvent clusters is important in the formation of secondary structure of proteins.[4] The excellent variation of the water-alcohol mixture dielectric constant make it an ideal solvent for many solutes.[3] The solvation of ethanol has therefore served as a model system to study the formation of a solvation sphere around a molecule that has a hydrophobic and a hydrophilic part.[5] Ethanol/water mixtures are non-ideal solutions with unusual physicochemical and thermodynamic properties such as negative excess entropy[6] and partial molar volumes[7].

The first study of the water-ethanol system can be found in the doctoral thesis of Dmitriy Mendeleev with the title 'Discourse on Alcohol and Water Mixing' in 1865[8], where he suggested that water and ethanol forms certain stable clusters (i.e. clathrate hydrates in current literature). There are number of experimental papers that support the existence of clathrate like structures in the ethanol/water mixture. In these clathrate like structures water develops a H-bonded network similar to ice, where each water molecule in the cage is tetrahedrally coordinated to 4 other water molecules.

Clathrate hydrate formation in water alcohol solutions was observed via light scattering with a structure of 21 water molecules.[9] Smaller cluster with 5-6 water molecules were observed through a dielectric relaxation technique (10^{+6}–10^{-3} Hz) and differential scanning calorimetry.[10] In a Raman scattering study the existence of clathrate hydrates was supported by the calculation of the H-bonding strength in ethanol-water mixtures which were maximum for 20 vol% ethanol.[11] A complex clustering mechanism of EtOH-water mixtures was observed through photothermal microfluidic cantilever deflection spectroscopy (PMCDS).[12] A ^{1}H-NMR study based on multivariate curve resolution came to the conclusion that ethanol-ethanol clusters exist above a critical concentration of ethanol in ethanol/water mixtures.[13]

The solvation of ethanol in water has also been studied computationally via Car-Parrinello molecular dynamics simulations which showed that ethanol can easily be accommodated in the hydrogen-bonded network of water molecules without altering its structure.[14] These structural features were in good agreement with neutron diffraction[15] and force field[16] molecular dynamics simulations the later giving no evidence of clathrate-like cages around the hydrophobic end of the alcohol. Molecular dynamics simulations of methanol in water have shown that the structure

of water is preserved, rather than enhanced, around hydrophobic groups and that water hydrogen-bonding to polar solute groups sacrifice solvent−solvent interactions to some degree.[17] In methanol-water mixtures it was found that the hydroxyl group mostly affects the structure of water and that water molecules are highly localised around the hydroxyl group.[18]

The evidence of clathrate structure of ethanol/water mixtures is therefore far from conclusive as little is known about the exact structure water has in it and whether it forms H-bonded networks around the hydrophobic part of the ethanol. Therefore further combined experimental and computational study is necessary. Here we have studied the experimental FTIR-ATR spectrum of x% v/v ethanol/water mixtures where x = 10, 20, 30, 40, 50, 60, 70, 80, 90 and 100. The spectral shifts in these FTIR-ATR spectra where interpreted using high-level hybrid DFT calculations in implicit and explicit water models. Furthermore, we have supported the existence of a H-bonded network around the ethanol molecule via molecular mechanics full optimisations in explicit water clusters with up to 30 water molecules.

2. Computational Methods

All density functional theory (DFT) calculations were performed within the Gaussian 09 suit of programs using the B3LYP[19,20] with an augmented correlation-consistent valence quadruple-zeta basis set, denoted as aug-cc-pVQZ(5d, 7f)[21-25], in implicit solvation using the polarizable continuum model (PCM) using the integral equation formalism variant (IEFPCM).[26,27] Partial charges on the atoms were found using the atomic polar tensor (APT) method. This charge population analysis has the advantage of being invariant with respect to changes to the coordinate system.[28]

The molecular mechanics (MM) simulations were performed within Avogadro with Merck's MMFF94s force field, using the steepest descent optimisation algorithm.[29]

3. Experimental Methods

Fourier transform infrared (FTIR) spectra were recorded on an attenuated total reflectance (ATR) spectrometer by Perkin Elmer (Spectrum two) with a diamond cell, with a MIR source (8000-30 cm^{-1}), a $LiTaO_3$ detector (15700-370 cm^{-1}), supplied with KBr windows. IR spectra were recorded between 600 and 4000 cm^{-1} at a

resolution of 1cm^{-1}. The IR data where not signal averaged and presented without any further data processing. The sample were liquid ethanol >= 99% and ultrapure water (18.18 mΩ·cm at 25°C) directly placed onto the ATR equipment. Ethanol/water mixtures where prepared in a 10 mL volumetric flask where they were mixed by means of a disposable dropper. A volume of 0.5 mL of the mixture was placed onto the ATR equipment for measurement.

4. Results and Discussion

4.1 Experimental results

In Fig. 1 we present a series of FTIR-ATR spectra that were recorded as a function of different volume fractions (x% v/v, T = 20 ^{o}C) of ethanol in water where x = 0, 20, 40, 60, 80 and 100. This spectrum was obtained in smaller increments of the volume fraction of ethanol in water (i.e. x% v/v where x = 0, 10, 20, 30, 40, 50, 60, 70, 80, 90 and 100, this corresponds to mole/mole % = 3.4, 7.7, 13.2, 20.6, 30.9, 46.4, 72.1, 123.7 and 278.2) but for better clarity only every second spectrum is plotted in Fig.1. The FTIR-ATR spectra represent a gradual transition from the IR absorption spectrum of ethanol to the absorption spectrum of water in which we attempt to identify the various shifts of the peaks done in Fig. 2. The spectra were recorded as soon as the mixtures where prepared by placing about 0.5 mL of the mixture onto the ATR cell for measurement. The ATR cell was cleaned between measurements by means of chem wipes and left to dry in air. In this procedure we could not observe any noticeable condensation of water from the atmosphere, which would affect the bands corresponding to water. The experimental spectrum contains certain absorption bands that correspond to ethanol and two broad bands that correspond to water. The water bands are positioned at about 1641 cm^{-1} and at 3355 cm^{-1}, which correspond to the bending vibration of the H-O-H angle and the stretching vibration of the O-H group, respectively. The later peak is clearly due to the superposition of at least two bands, one asymmetric and one symmetric stretching band according to our calculated vibrational IR frequencies of water. Further spectral components may arise due to strongly and weakly H-bonded -OH groups and OH groups that are not H-bonded.[30]

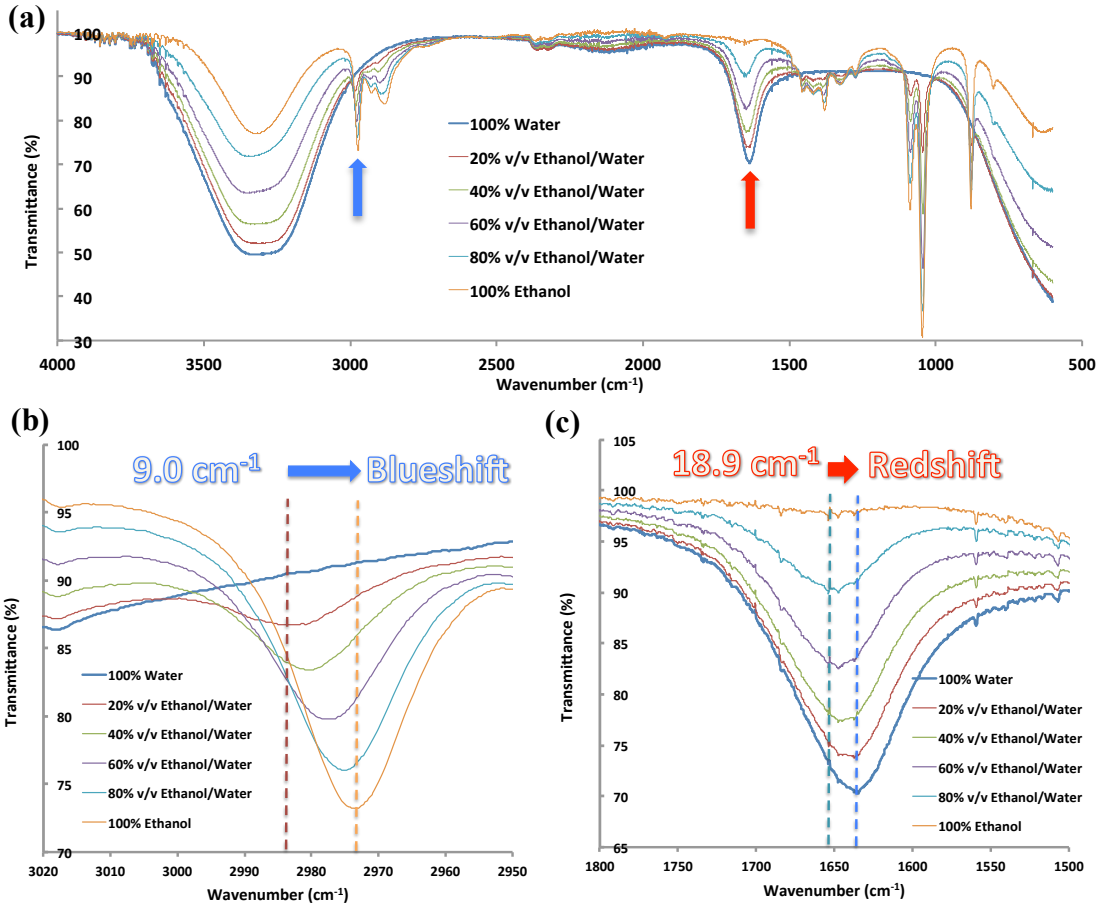

Fig. 1 FTIR-ATR spectra of ethanol/water mixtures from (a) 4000 to 500 cm^{-1}, (b) 3700-2800 cm^{-1} and (c) 1800-800 cm^{-1}. The red arrow indicates which peak had a redshift and blue arrow which peaks had a blueshift as a function of water content.

Between 3000 cm^{-1} and 2900 cm^{-1} ethanol has at least 4 bands in the experimental IR spectrum as shown in Fig. 1. These vibrational bands correspond to the C-H asymmetric stretch of β-CH_3, C-H symmetric stretch of β-CH_3, C-H asymmetric stretch of α-CH_2 and C-H symmetric stretch of α-CH_2 starting from the higher frequency and going to the lower frequency bands. The corresponding peaks can be found in the calculated IR spectrum of ethanol between 3093 cm^{-1} - 2993 cm^{-1} according to Table 1. In the region of 1400-1300 cm^{-1} there are multiple peaks which

correspond to C-H bend of α-CH_2 and β-CH_3. These peaks can be found in the calculated spectrum of ethanol in Table 1 between 1523-1403 cm^{-1}. Following these, two intense peaks appear at 1086 cm^{-1} and 1044 cm^{-1} which correspond to O-H bending coupled to C-O stretching vibrations and O-H bending coupled to C-C stretching vibrations, respectively. These vibrations are found in the calculated spectrum between 1086 cm^{-1} and 1027 cm^{-1} in excellent agreement with the experimental values. The last band that can be observed to belong to ethanol is a band at 878 cm^{-1}, which corresponds C-C stretching vibrations. This band appears very close in the calculated spectrum in Table 1 at 889 cm^{-1}. We therefore, find qualitative agreement between experimental and calculated IR spectra of ethanol/water mixtures.

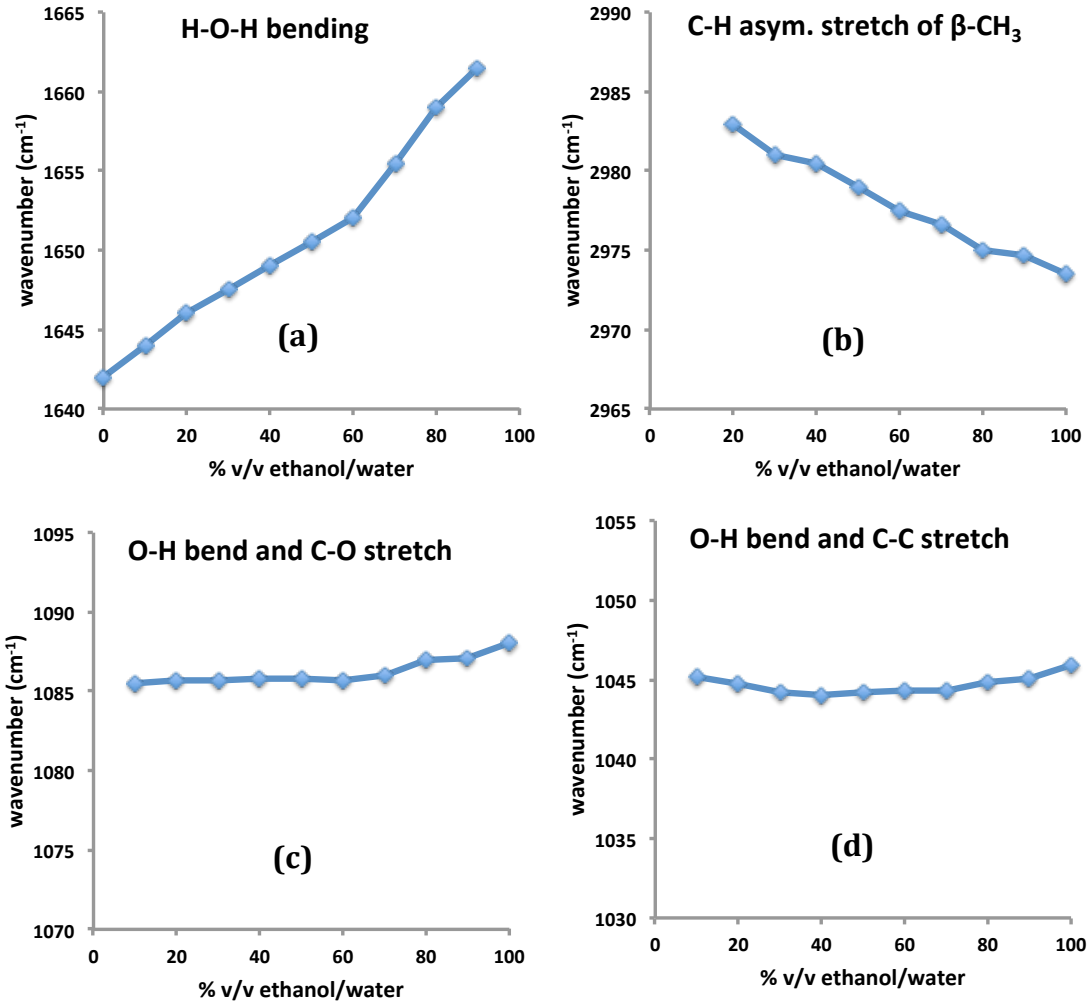

Fig. 2 Spectral shifts of peaks observed in FTIR-ATR spectra of ethanol/water mixtures of (a) H-O-H bending vibration, (b) C-H asymmetric stretching of β-CH_3, (c) O-H bending and C-O stretching vibration and (d) O-H bending and C-C stretching vibrations.

The peak in the water IR absorption spectrum that shows the greatest redshift with the increase of the water content is the peak at that corresponds to the bending vibration of H-O-H. The exact peak position of this band is plotted in Fig. 2(a) and it shows a redshift of 18.9 cm^{-1}. These shifts of the vibrational bands can be attributed to variations of the H-bonded network formed or could be evidence of a clathrate hydration of ethanol and water mixtures.[10,11,31] We attempt to explain this redshift via DFT calculations in the following section. The second band (see Fig. 2b) that appears to have a blueshift as a function of the water content in the mixture is the band that corresponds to the asymmetric stretching vibrations of the methyl group. This band gradually blueshifts from 2974 cm^{-1} to 2983 cm^{-1} as a function of the water content in the mixture. This could also be a result of clathrate hydration of the methyl group of ethanol.[10,11,31] The third band (see Fig. 2c) that has a small redshift as a function of the water content in the mixture is the combined O-H bend and C-O stretch mode, which redshifts by 2.54 cm^{-1}. The small shifts of this band indicate that the hydroxyl group of ethanol changes little environment as the content of water increases. This maybe due to the incorporation of the O-H group in the cyclic H-bonded network of water molecules as we later show via molecular mechanics simulations. The same interpretation can be given to the fourth band (see Fig. 2d) of the FTIR-ATR spectrum which changes by less than 2 cm^{-1}. This band corresponds to a coupled O-H bending vibration and C-C stretching vibration.

4.2 Computational Results

With the B3LYP/aug-cc-pVTQZ method we have fully optimised the structures of (i) a water molecule with water as the solvent, (ii) a water molecule with ethanol as a solvent (infinite dilution of water in ethanol), (iii) an ethanol molecule with ethanol as the solvent and (iv) an ethanol molecule with water as the solvent and calculated the IR spectrum of each model. In the simulation of model (iii) the peak at 1086 cm^{-1} appears at 1085.67 cm^{-1} (ethanol as solvent) and is a bending vibration of the angle of the -OH group in ethanol. This peak redshifts to 1085.18 cm^{-1} when water is the solvent (model iv). This can explain the redshift of the band in Fig. 2c at 1088.07 cm^{-1} to 1085.51 cm^{-1} which can be entirely attributed to the fact that the O-H bond in ethanol vibrates in a bending motion at slightly lower wavenumbers when the relative permittivity of the solvent changes from 24.3 (in ethanol) to 80.2 (in water) at

20 ^{o}C.[32] This solvent effect can also be seen in the calculated atomic polar tensor (APT) charges of ethanol which are depicted in Fig. 3.

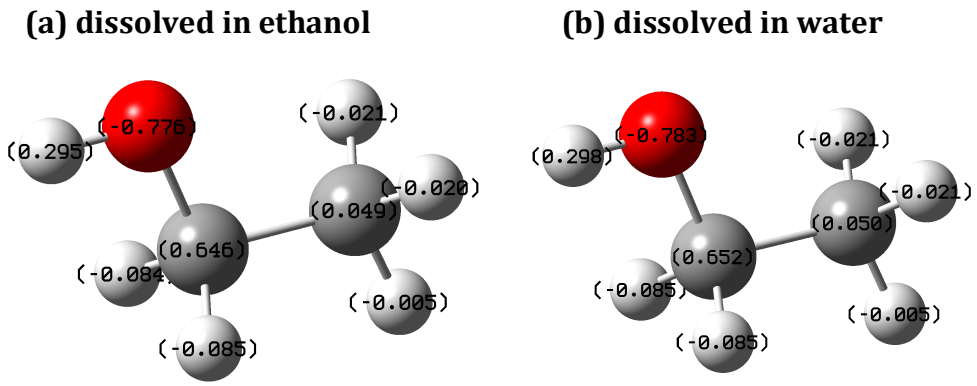

Fig. 3 Calculated APT charges of ethanol when (a) dissolved in ethanol and (b) dissolved in water.

These charges are the same on the β-CH_3 carbon atom that is bound to carbon and all hydrogens bound directly to carbon. But they differ or the C-O-H group, which defines the angle that vibrates in the simulated IR spectrum of ethanol. The charges of these atoms become slightly greater when the solvent changes from ethanol to water. In particular, the charge on the H changes from 0.295 to 0.298, the charge of O changes from -0.776 to -0.783 and the charge of C changes from 0.646 to 0.652. This clearly suggests that the solvation alters the charges on the atoms of just the C-O-H group and that these changes are observable in the redshift of the IR spectrum of the 1086 cm^{-1} peak. The higher charges with water as a solvent indicate that the force constant for the vibration of this angle will decrease if we just consider a point charge model for this bond that vibrates in a bending motion. A smaller bond angle force constant would suggest also smaller vibrational frequency of this bond when the solvent becomes from ethanol, water.

The calculated values for infrared frequency (ν_{IR}), infrared intensity (I_{IR}), bond length (r) and bond angle (φ) for ethanol using the B3LYP /aug-cc-pVQZ method and ethanol solvation via the IEFPCM model are tabulated in Table 1. We observe qualitative agreement with the IR absorption bands observed experimentally that are shown in Fig. 1. The most drastic difference was the peak for the O-H stretching

vibration, which is significantly overestimated due to the lack of hydrogen bonding when the vibrational frequency of a plain water molecule is calculated.

Table 1 Calculated values for the infrared frequency (ν_{IR}), infrared intensity (I_{IR}), bond length (r) and bond angle (φ) for ethanol using the B3LYP /aug-cc-pVQZ method and ethanol solvation via the IEFPCM model.

Vibrational mode	**Frequency** (cm^{-1})	**Intensity** (10^{-40} esu^2 cm^2)	**Bond length** (Å)	**Bond angle** (°)
O-H stretch	3818	59	0.961	108.6
C-H asym. stretch of β-CH_3	3093	75	1.090	108.5
C-H sym. stretch of β-CH_3	3028	31	1.090	108.3
C-H asym. stretch of α-CH_2	3019	71	1.094	107.8
C-H sym. stretch of α-CH_2	2993	114	1.094	107.8
C-H bend of α-CH_2 and β-CH_3	1523-1403	>42	-	-
O-H bend	1261	271	0.961	108.6
O-H bend and C-O stretch	1086	125	0.961	108.6
O-H bend and C-C stretch	1027	403	0.961	108.6
C-C stretch	889	114	1.513	108.4
O-C-C bend	418	150	-	108.4
O-H bend and β-CH_3 rotation	275-237	1155-1523	-	-

The other peak that showed a more pronounced redshift when dissolvation in water occurs was the peak centered at 1645 cm^{-1}, which corresponds to the H-O-H bending vibration. This peak redshifts by 18.9 cm^{-1} and from our previous analysis for the 1086 cm^{-1} of ethanol this could not be attributed to a simple solvent dielectric effect that occurs when going from ethanol as the solvent to water as the solvent. The significant peak redshift of 18.9 cm^{-1} can only be explained by a water/ethanol model that has also H-bonding networks or the existence of clathrate hydrates.[10,11,31] In order to understand better this redshift we have performed DFT calculations with the hybrid B3LYP[19,20] functional using the augmented correlation-consistent quadruple valence zeta basis set (i.e. aug-cc-pVQZ).[21-25] Initially, we simulated the IR spectrum of a single water molecule in water as the solvent and in ethanol. The IR spectrum of water just gave three absorption bands, which are tabulated in Table 2. The highest in wavenumber bands correspond to the symmetric and asymmetric stretching vibration of O-H groups which in the experimental spectrum in Fig. 1 is the broad band centered at 3355 cm^{-1} which is a broad band due to H-bonding. The H-bonds significantly lower the vibrational frequency of the stretching of O-H as this is

calculated in the isolated molecule. This indicates that water forms a strong H-bonded network and possibly stable water clusters, the stability of which weakens the O-H bond strength, resulting in lower experimental vibrational frequencies than the calculated ones.

From the calculated vibrational frequency of the H-O-H bending mode that are shown in Table 2, it can be seen that it decreases only by 0.3 cm^{-1} going from ethanol as a solvent to water. This cannot explain the 18.9 cm^{-1} redshift found experimentally which may only be explained by considering H-bonded networks or the existence of clathrate hydrates.[10,11,31] The presence of an enhanced H-bonded network or the existence of clathrate hydrates could explain the 18.9 cm^{-1} redshift of the vibrational bending mode of water as the water content increases. The increased water content will be less disrupted by the presence of ethanol molecules, which means that a denser H-bonded network or clathrate like structure could be formed. In this structure the strength of the H-bonds will be greater than the strength of the H-bonds in water hydrating ethanol. A greater strength of the H-bonding interactions would mean that the corresponding H-bonded O-H groups will have weaker O-H bonds. Weaker O-H bonds means that the bending force constant will decrease, observing therefore lower vibrational frequencies of the O-H bending vibration in water and the observed redshift of the band observed in Fig. 2a.

Table 2 Calculated values for the infrared frequency (ν_{IR}), infrared intensity (I_{IR}), bond length (r) and bond angle (φ) (i) for water H-bonded to ethanol in implicit ethanol as the solvent, (ii) for water in an implicit solvent of ethanol, (iii) for water in in an implicit solvent of water and (iv) for the water dimer in an implicit solvent of water using the B3LYP /aug-cc-pVQZ method. Values in parenthesis are average values.

Vibrational mode	**Frequency** (cm^{-1})	**Intensity** (10^{-40} esu^2 cm^2)	**Bond length** (Å)	**Bond angle** (°)
*i) in **ethanol** water H-bonded to ethanol (water-ethanol)*				
H-O-H bending	1621.10	239	0.96237	105.175
O-H sym. stretch	3788.1	22	-	-
O-H asym. stretch	3876.73	133	-	-
*ii) in **ethanol** as solvent (implicit)*				
H-O-H bending	1619.20	248	0.96179	104.646
O-H sym. stretch	3793.51	18	-	-
O-H asym. stretch	3882.10	106	-	-
*iii) in **water** as solvent (implicit)*				
H-O-H bending	1618.92	252	0.96186	104.617
O-H sym. stretch	3792.9	19	-	-
O-H asym. stretch	3880.85	111	-	-
*iv) in **water** water dimer H-bonded (water-water)*				
H-O-H bending	(1628.70)	(227)	(0.96804)	(105.151)
O-H sym. stretch	(3739.70)	(22)	-	-
O-H asym. stretch	(3873.88)	(134)	-	-

In Table 2 the vibrational frequencies of water have been calculated for various environments. Namely (i) for water H-bonded to ethanol in ethanol as the solvent which corresponds to the infinite dilution of water in ethanol (e.g. 99.9% v/v ethanol/water), (ii) for water in ethanol as the solvent which corresponds to the infinite dilution of water in ethanol, with water not forming H-bonds (e.g. 99.9% v/v ethanol/water), (iii) for water in water as the solvent (omitting the existence of H-bonds) which corresponds to the infinite dilution of ethanol in water (e.g. 0.1% v/v

ethanol/water) and (iv) for water H-bonded to another water molecule in water as the solvent which corresponds to pure water. Going from (i) to (iv) the water content increases which blueshifts the bending stretching vibration of water bending vibration from 1621.10 cm^{-1} to 1628.70 cm^{-1}. This computationally determined blueshift contradicts with the experimentally found redshift from 1654 cm^{-1} to 1637 cm^{-1} shown in Fig. 2a. This suggests that the redshift determined experimentally for the vibrational band of water as the water content increases has to be a result of other ordering phenomena in the ethanol-water mixture, such as the formation of clathrate hydration clusters and it cannot be entirely attributed to an increase of the H-bonded network as the content of water increases in the mixture.

4.3 A theoretical model of ethanol/water mixtures

We propose a theoretical model for the spectral shifts observed in ethanol/water mixtures, which is based on the simplified schematic in Fig. 4. It is closely related to the existence of a hydrophobic effect in ethanol/water mixtures which depends on the size and branching of the hydrocarbon chain in the alcohol.[33] This hydrophobic effect causes the O-H bonds of adjacent water molecules to the ethanol, to not directly point their O-H bonds towards the β-CH_3 group of ethanol. Furthermore, the model considers ethanol molecules that are isolated and do not H-bond in mixtures that are water rich in agreement with MD simulations of water/ethanol mixtures.[34] The model does not describe the mixtures with high ethanol content where some form of aggregation of ethanol has been found via small angle neutron scattering of D_2O-ethanol solutions.[35] It is in agreement with ethanol/water compressibility studies that reached the conclusion that water is stabilised in an ordered, less dense and rigid structure around the solute molecule.[36] It also does not exclude the possibility of the formation of "icebergs" in which solute molecules form small frozen patches of water.[37]

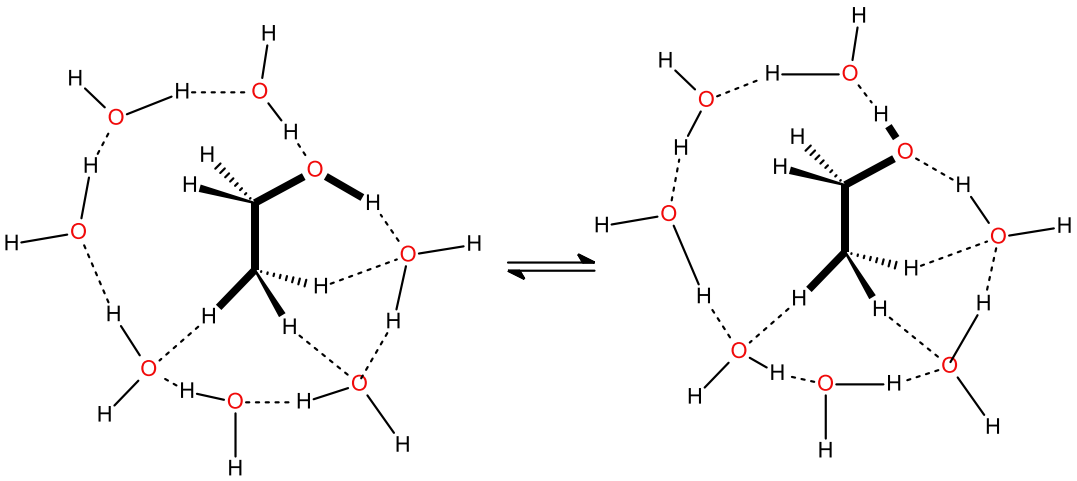

Fig. 4 Simplified schematic that shows the formation of the H-bonded network around each ethanol molecule and the interaction of the methyl group hydrogens with the surrounding oxygens of water when the water content of the ethanol/water mixture is high.

As water becomes more in the ethanol/water mixture there is a more complete formation of a H-bonded network around ethanol molecules. This H-bonded network[3] reduces the strength of the O-H bond due to H-bonding. This makes the bending vibration of the O-H bond to become weaker which may explain the redshift of the 1645 cm^{-1} by 18.9 cm^{-1}. Simultaneously, as the H-bonded cluster forms around the hydrophobic methyl group of ethanol the C-H bonds become stronger as they are attractively pulled to a smaller extent by the surrounding oxygen atoms of water, which have a smaller negative partial charge, due to the H-bonded network (and presumable H-tunneling which can be seen by going from the cyclic H-bonded network on the left to the H-bonded network to the right in Fig. 4) around each ethanol molecule. This may explain the blueshift of 9.0 cm^{-1} of the vibrational stretching frequency of the C-H bond of the β-CH_3 group. Therefore, both infrared shifts that we observed in this study are consistent with the formation of a cage-like cyclic structure of water molecules around each ethanol, which is H-bonded to the ethanol molecule. This is not the first account of the formation of cage like water cluster around ethanol molecules in water. In particular, many previous studies have found that there is an existence of clathrate structures in ethanol/water mixtures, which was attributed to a hydrophobic effect. A 21 water molecule clathrate hydrate formation in water alcohol solutions was observed via light scattering.[9] A dielectric

relaxation technique (10^{+6}–10^{-3} Hz) and differential scanning calorimetry observed smaller clusters with 5-6 water molecules.[10] In a Raman scattering study the existence of clathrate hydrates was supported by the calculation of the H-bonding strength in ethanol-water mixtures which were maximum for 20 vol% ethanol.[11] Photothermal microfluidic cantilever deflection spectroscopy (PMCDS) found a complex clustering mechanism in EtOH-water mixtures.[12] In this study we provide evidence from molecular simulations that a cyclic H-bonded network between ethanol and about 7 water molecules exists which are H-bonded in a structure that is depicted in the simplified schematic of Fig. 4.

In the simplified model proposed hydrogen in the H-bonded network can exhibit H-tunneling which is also supported by recent NMR studies of ethanol/water mixtures that show that the peaks of the alcohol hydroxyl group and that of water are indistiguishable unless the temperature is below -10 °C.[38] In addition, the existence of H-bonded networks in ethanol/water mixtures has been previously observed via partial molar Raman spectroscopy.[39]

Based on the simplified model depicted in Fig. 4 we have tested whether stable cyclic structures of water exist around ethanol using the MMFF94s force field (FF). This FF is particularly efficient in identifying H-bonded networks in water without significant computational cost. We have performed simulations with as many as one ethanol molecule surrounded by 30 water molecules that formed a H-bonded cage around the ethanol molecule (see Fig. 5(a)) which was formed by randomly placing water molecules around an ethanol molecule. In this cage most water molecules, especially the ones that lie close to the methyl group are in a square H-bonded arrangement, which occasionally also had pentagonal H-bonded networks and very rarely a hexagonal H-bonded network. These cyclic H-bonded networks form readily around the hydrophobic part of ethanol. We have then removed water molecules one by one, optimising the structure after each succesive removal of a water molecule. Our aim was to expose in the water H-bonded cage of the ethanol-water cluster the H-bonded network that appears in structure similar to what is depicted in Fig. 4. We were able to isolate and ethanol-$(H_2O)_8$ cluster which had a cyclic H-bonded structure shown in Fig. 5(b). We then attempted to see whether this cyclic structure represent the minimum number of water molecules that can form a cyclic H-bonded structure around ethanol and found that smaller cyclic structures that contain 7 and 6 water molecules could also exist, shown in Fig. 5(c) and Fig. 5(d),

respectively. The simulations performed provide evidence that H-bonded[29] network around the ethanol molecule exist in these simulations based on molecular mechanics and that it should be further tested whether H-tunneling can occur in these cyclic H-bonded networks. It is intriguing that the findings by Nishi et al. who performed mass spectroscopic studies on ethanol-water mixtures and found evidence of ethanol monomers that are followed by long water sequences of hydrated species of the form $C_2H_5OH(H_2O)_n$ when $x_E < 0.04$ which is in agreement with the ethanol-water structures suggested here.[40,41]

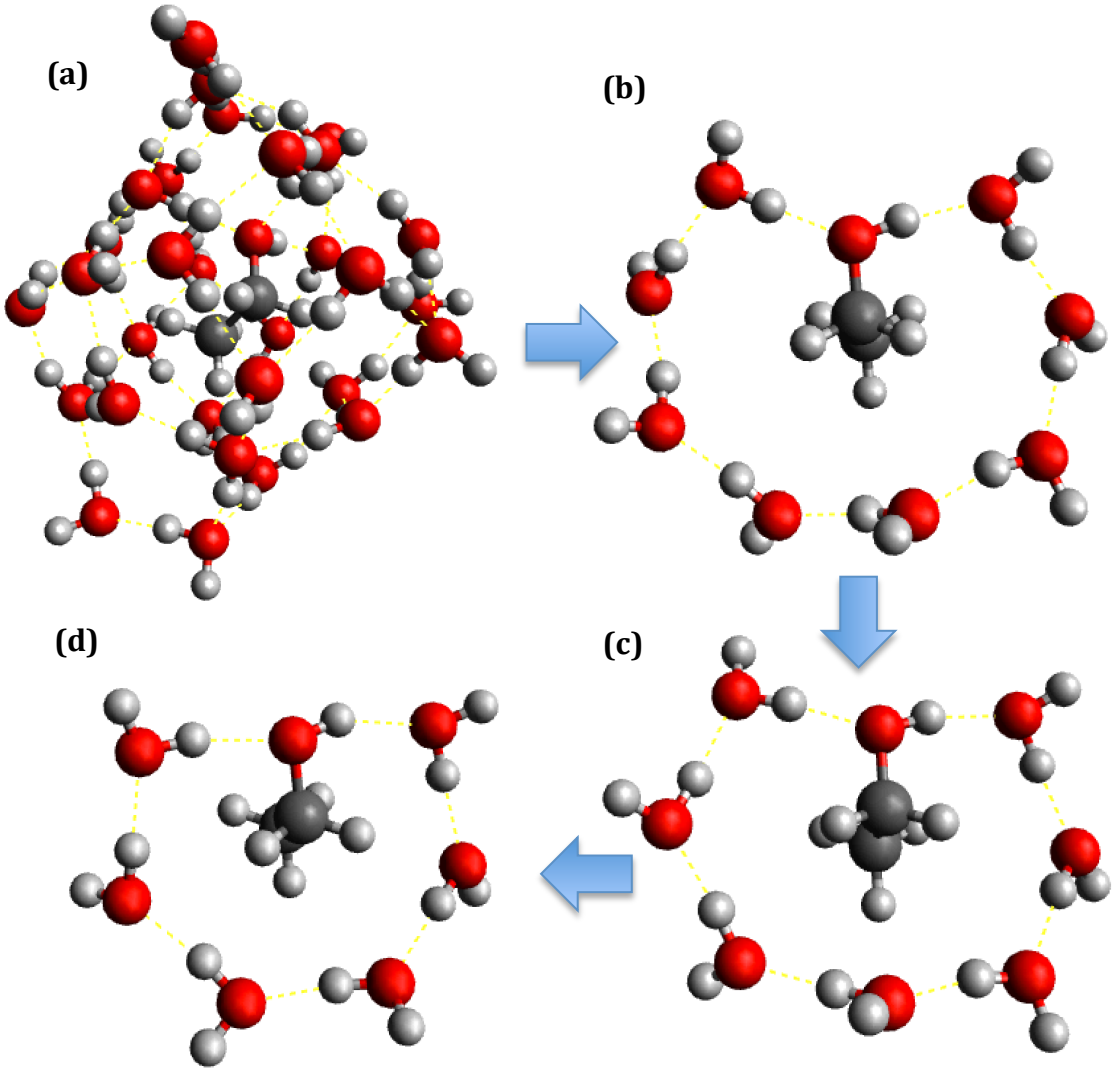

Fig. 5 Optimised structures with the MMFF94s force field of the ethanol-water clusters. The (a) ethanol-$(H_2O)_{30}$, (b) ethanol-$(H_2O)_8$, (c) ethanol-$(H_2O)_7$ and (d) ethanol-$(H_2O)_6$ coordinates are given in the supporting information file as S-Fig. 1, S-Fig. 2, S-Fig. 3 and S-Fig. 4, respectively.

5. Conclusions

Our experimental FTIR-ATR study of the ethanol/water mixtures, molecular mechanics and hybrid density functional theory calculations and infrared simulations are supportive of the existence of a strong structural change in the water/ethanol mixture as the solvent changes from ethanol to water. These structural changes are accompanied by a redshift of 18.9 cm^{-1} of the vibrational bending band of the H-O-H bond angle of water and a blueshift of 9.0 cm^{-1} of the C-H stretching band of the β-CH_3. DFT calculations with implicit and explicit solvent show that a small red-shift of 2 cm^{-1} could only be expected on the basis of changes in the dielectric constant of the solvent, in water/ethanol mixtures as the mixture is diluted with water. The spectral changes of the FTIR-ATR bands are explained through a simplified model that invokes the presence of a cyclic H-bonded network around each ethanol molecule, which is confirmed through molecular mechanics simulations with ethanol dissolved in explicit water clusters.

Availability of data

The data that supports the findings of this study are available within the article and its supplementary material.

Acknowledgements

Computation for the work presented in this paper was supported by the University of Greenwich high performance computer resources (https://www.gre.ac.uk/it-and-library/hpc). The authors acknowledge access to research facilities at the school of science at the University of Greenwich.

References:

[1] D. Eisenberg and W. Kauzmann,The Structure and Properties of Water, Clarendon, Oxford, 1969.

[2] Structure of Water and Aqueous Solutions, edited by W. A. P. Luck, Verlag Chemie-Physik, Weinheim, Germany, 1974.

[3] F. Franks, D.J.G. Ives, Q. Rev. Chem. Soc. 20 (1966) 1.

[4] D.-P. Hong, M. Hoshino, R. Kuboi, Y. Goto, J. Am. Chem. Soc. 121 (1999) 8427.

[5] M. Ikeguchi, S. Shimizu, S. Nakamura, K. Shimizu, J. Phys. Chem. B 102 (1998) 5891.

[6] A.K. Soper, L. Dougan, J. Crain, J.L. Finney, J. Phys. Chem. B 110 (2006) 3472.
[7] H.S. Franks, M.W. Evans, J. Chem. Phys. 13 (1945) 507.
[8] D.I. Mendeleev, Discourse on Alcohol and Water Mixing, Akad. Nauk SSSR, Moscow, p.381, 1959.
[9] K. Iwasaki, T. Fujiyama, J. Phys. Chem. 81 (1977) 1908.
[10] S.S.N. Murthy, J. Phys. Chem. A 103 (1999) 7927.
[11] T.A. Dolenko, S.A. Burikov, S.A. Dolenko, A.O. Efitorov, I.V. Plastinin, V.I. Yuzhakov, S.V. Patsaeva, J. Phys. Chem. A 119 (2015) 10806.
[12] M.S. Ghoraishi, J.E. Hawk, A. Phani, M.F. Khan, T. Thundat, Sci Rep 6 (2016) 23966.
[13] N. Hu, D. Wu, K.J. Cross, D.W. Schaefer, Appl. Spectrosc. 64 (2010) 337.
[14] T.S. van Erp, E.J. Meijer, J. Chem. Phys. 118 (2003) 8831.
[15] J. Turner, A.K. Soper, J. Chem. Phys. 101 (1994) 6116.
[16] J. Fidler, P.M. Rodger, J. Phys. Chem. B 103 (1999) 7695.
[17] E.C. Meng, P.A. Kollman, J. Phys. Chem. 100 (1996) 11460.
[18] A. Laaksonen, P.G. Kusalik, I.M. Svishchev, J. Phys. Chem. A 101 (1997) 5910.
[19] A.D. Becke, J. Chem. Phys. 98 (1993) 5648.
[20] C. Lee, W. Yang, R.G. Parr, Phys. Rev. B 37 (1988) 785.
[21] D.E. Woon, T.H. Dunning Jr., J. Chem. Phys. 98 (1993) 1358.
[22] A. Wilson, T. van Mourik, T.H. Dunning Jr., J. Mol. Struct. 388 (1996) 339.
[23] K.A. Peterson, D.E. Woon, T.H. Dunning Jr., J. Chem. Phys. 100 (1994) 7410.
[24] R.A. Kendall, T.H. Dunning Jr., J. Chem. Phys. 96 (1992) 6796.
[25] T.H. Dunning Jr., J. Chem. Phys. 90 (1989) 1007.
[26] S. Miertuš, E. Scrocco, J. Tomasi, Chem. Phys. 55 (1981) 117.
[27] J.L. Pascual-ahuir, E. Silla, I. Tuñon, J. Comp. Chem. 15 (1994) 1127.
[28] J. Cioslowski, J. Am. Chem. Soc. 111 (1989) 8333.
[29] M.D. Hanwell, D.E. Curtis, D.C. Lonie, T. Vandermeersch, E. Zurek, G.R. Hutchison, Journal of Cheminformatics 4 (2012) 17.
[30] S. Burikov, S. Dolenko, T. Dolenko, S. Patsaeva, V. Yuzhakov, Molecular Physics 108 (2010) 739.
[31] S. Burikov, T. Dolenko, S. Patsaeva, Y. Starokurov, V. Yuzhakov, Molec. Phys. 108 (2010) 2427.
[32] G.G. Archer, P. Wang, J. Phys. Chem. Ref. Data 19 (1990) 371.
[33] J. Catalán, C. Díaz-Oliva, F. García-Blanco, Chem. Phys. 527 (2019) 110467.
[34] C. Zhang, X. Yang, Fluid Ph. Equilibria 231 (2005) 1.
[35] G. D'Arrigo, J. Teixeira, J. Chem. Soc., Faraday Trans. 86 (1990) 1503.
[36] G. D'Arrigo, A. Paparelli, J. Chem. Phys. 88 (1988) 405.
[37] H.S. Frank, M.W. Evans, J. Chem. Phys. 13 (1945) 507.
[38] M. Matsugami, R. Yamamoto, T. Kumai, M. Tanaka, T. Umecky, T. Takamuku, J. Mol. Liq. 217 (2016) 3.
[39] S. Stehle, A.S. Braeuer, J. Phys. Chem. B 123 (2019) 4425.
[40] N. Nishi, K. Koga, C. Ohshima, K. Yamamoto, U. Nagashima, K. Nagami, J. Am. Chem. Soc. 110 (1988) 5246.
[41] N. Nishi, S. Takahashi, M. Matsumoto, A. Tanaka, K. Muraya, T. Takamuku, T. Yamaguchi, J. Phys. Chem. 99 (1995) 462.